

KERNFORSCHUNGSZENTRUM

KARLSRUHE

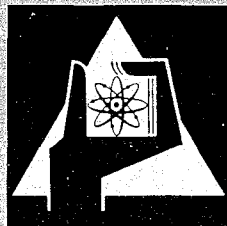
Januar 1968

KFK 744

Institut für Angewandte Kernphysik

A "Grey" Neutron Detector for the Intermediate Energy Region

W.P. Pönitz



GESELLSCHAFT FÜR KERNFORSCHUNG M. B. H.

KARLSRUHE

A "GREY" NEUTRON DETECTOR FOR THE INTERMEDIATE ENERGY REGION

W. P. PÖNITZ*

Institut für Angewandte Kernphysik, Kernforschungszentrum Karlsruhe

Received 13 August 1967

A neutron detector for the accurate measurement of relative neutron flux intensities in the keV energy region is described. The detector consists, in its simplest arrangement, of a paraffin pile and a NaI(Tl) detector to detect the 2.2 MeV capture γ -rays. The

efficiency curve is relatively flat in the considered energy range. The efficiency curve depends only slightly on a change in the parameters used for its calculation. The application of the detector in neutron cross section experiments is described.

1. Introduction

There exist already several fast neutron detectors based upon the slowing down of fast neutrons and measuring of the thermalized neutrons. The best-known detector of this type is the "long counter" as described by Hanson and McKibben¹⁾ and by McTaggart²⁾. Some other detectors of this kind are the "paraffin pile"³⁾, the "graphite sphere"³⁾, the "boron pile"⁴⁾ and the "large liquid scintillator"³⁾. The first two detectors are heterogeneous systems, as is the long counter, and they are therefore more sensitive to a neutron field variation than a homogeneous system. The latter two detectors are homogeneous and have large efficiencies. However, these facilities are relatively expensive. Moreover, in the case of the large liquid scintillator the background problem plays an important rôle.

In the present paper an improved form of the "grey neutron detector", [Pönitz and Wattecamp⁵⁾] will be described and its properties will be discussed. It will be shown that this detector allows accurate neutron beam intensity measurements in the energy range from zero to a few MeV. This is possible even though the detector is a very simple facility consisting of a paraffin (or water) sphere (or pile) and a NaI(Tl) detector.

2. The principle of the detector

We first consider an isotropically emitting neutron source in the center of a water or paraffin sphere. A NaI(Tl) detector is located at the edge of the sphere as shown in fig. 1. The source neutrons are slowed down in the moderator. A part of the thermalized neutrons is captured in the hydrogen, and another part leaks out of the sphere. An increase in the primary neutron energy results in a stronger leakage of neutrons. The neutron capture events are the sources of the 2.2-MeV γ -rays some of which are detected by the NaI(Tl) detector.

In order to understand the basic principle of the detector, we make two additional assumptions:

a. The radius of the sphere should be large enough

that all neutrons are slowed down and captured in the moderator (no leakage).

b. There should be no γ -ray absorption in the sphere.

With these assumptions and neglecting the capture in components of the moderator other than hydrogen, the 2.2-MeV γ -ray flux integrated over the surface of the sphere is independent of the primary neutron energy of the source and equal to the neutron source strength. This means that the efficiency of the detector will be expected to be a constant. Due to this important basic principle of the detector, calculated efficiency curves taking into account the γ -ray absorption in the sphere are very reliable as long as no neutron leakage occurs.

* Now at Argonne Nat. Lab., Argonne, Illinois, U.S.A.

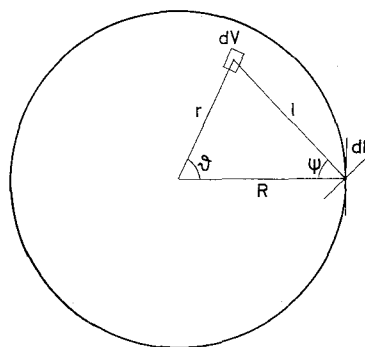
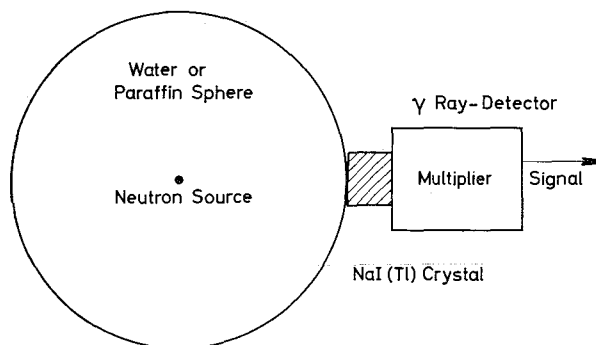


Fig. 1. Principle of the detector.

3. Calculation of the efficiency curve of the detector

We intend to measure only the photopeak of the 2.2-MeV capture γ -ray which simplifies considerably the calculation of the efficiency of the detector.

The γ -ray intensity going through a surface element dF of the sphere and originating in the volume element dV (fig. 1) is

$$\int_0^{E_0} \Sigma_a(E) \cdot \phi(r; E, E_0) dE \cdot \{(e^{-\mu l}) / (4\pi l^2)\} \cos\psi d\cos\vartheta d\varphi r^2 dr. \quad (1)$$

$\phi(r; E, E_0)$ is the neutron flux in the sphere at the radius r and energy E , depending on the primary neutron source energy E_0 and the radius R of the sphere. $\Sigma_a(E)$ is the macroscopic capture cross section of hydrogen in the moderator. μ is the total attenuation coefficient for the 2.2-MeV capture γ -rays in the moderator. The quantities l , ψ , ϑ , φ and r are shown in fig. 1. The energy integral of the first two terms in eq. (1) gives the radius dependent capture rate which we assume to be proportional to the thermal neutron flux. Thus we get for the efficiency η of the detector

$$\eta \sim \int_{r=0}^R \int_{x=1}^{-1} l^{-2} e^{-\mu l} \cos\psi dx \cdot r^2 \phi_{th}(r) dr, \quad (2)$$

where $x = \cos\vartheta$, $l = [R^2 + r^2 - 2Rrx]^{1/2}$ and $\cos\psi = (R - rx)/l$. R is the radius of the sphere.

Because of the principle of the detector, we can expect that the particular choice of $\phi_{th}(r)$ should not have a strong influence on the calculated efficiency curve as long as no leakage occurs. We verify this using three different flux functions:

A. The thermal neutron flux was calculated with age theory [ref. 6], p. 164] assuming an infinite medium giving the result

$$\phi_{th}(r) \sim r^{-1} e^{-r/L^2} \{e^{-r/L} [1 + \operatorname{erf}(\frac{1}{2}r\tau^{-1/2} - \tau^{1/2}/L)] - e^{r/L} [1 - \operatorname{erf}(\frac{1}{2}r\tau^{-1/2} + \tau^{1/2}/L)]\}. \quad (3)$$

B. The thermal neutron flux was calculated with a two neutron group theory [ref. 6], p. 164] for an infinite medium giving

$$\phi_{th}(r) \sim (L^2 - \tau)^{-1} r^{-1} \{\exp(-r/L) - \exp(-r/\tau^{1/2})\}, \quad (4)$$

where L is the diffusion length and τ the Fermi age.

C. The thermal neutron flux was calculated using age theory [ref. 6], p. 165] assuming a finite sphere with a radius R yielding

$$\phi_{th}(r) \sim \sum_m^{\infty} m \{1 + (m\pi L/R)^2\}^{-1} \cdot [\exp\{- (m\pi\tau^{1/2}/R)^2\}] r^{-1} \sin(m\pi r/R). \quad (5)$$

Fig. 2 shows the efficiency curves calculated with eq. (2) and the different neutron flux functions as given in eqs. (3)–(5). The curves are normalized at 30 keV.

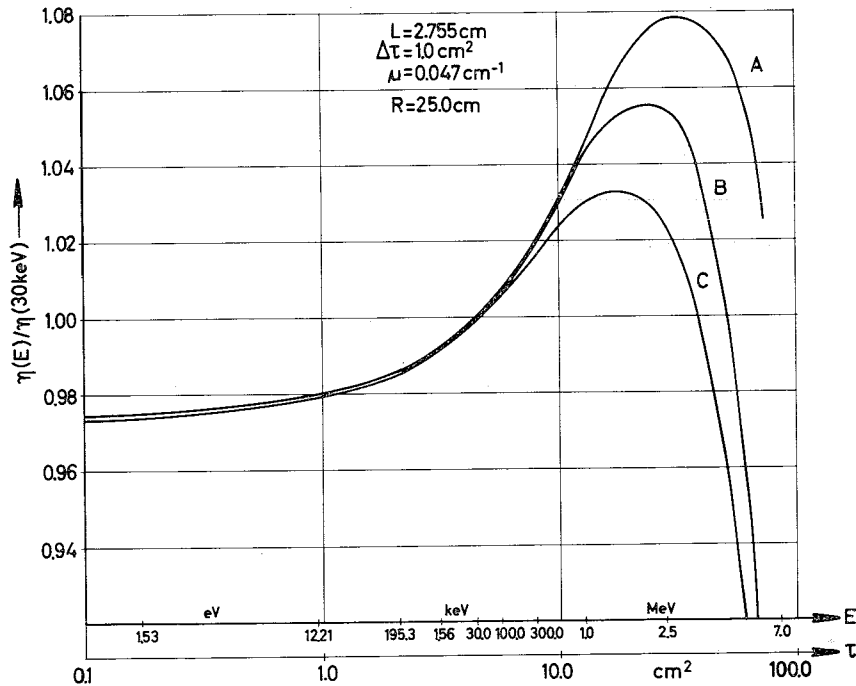


Fig. 2. The efficiency of the detector vs energy calculated for different thermal neutron flux functions.

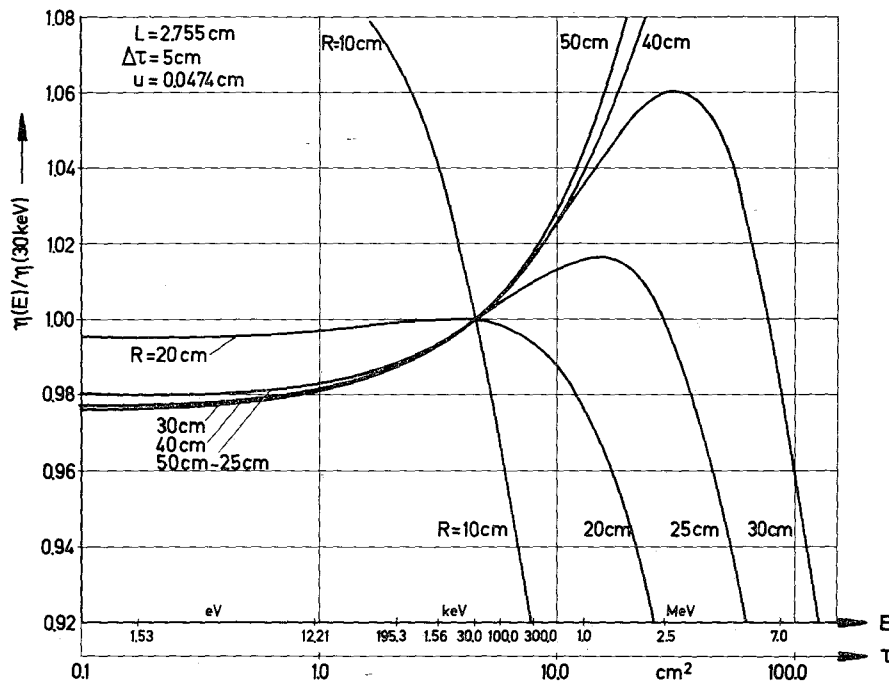


Fig. 3. The efficiency of the detector vs energy. The variable parameter is the radius of the water sphere.

The result confirms the expected feature of this detector. The three curves are in agreement below a few hundred keV primary neutron energy where the neutron leakage is very small for a water sphere with $R = 25.0 \text{ cm}$.

4. Influence of the parameters

The calculated efficiency curves depend on the parameters R, μ, L and $\Delta\tau$ where $\tau = \Delta\tau + \tau_{1.44 \text{ eV}}$. $\tau_{1.44 \text{ eV}}$ is the age of the neutrons at the energy of the indium

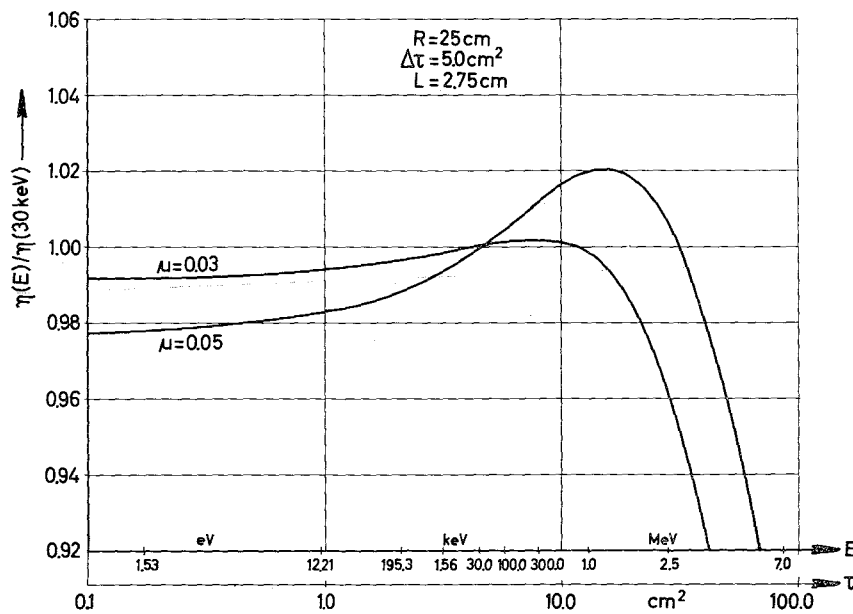


Fig. 4. The efficiency of the detector vs energy. The variable parameter is the γ -ray attenuation coefficient.

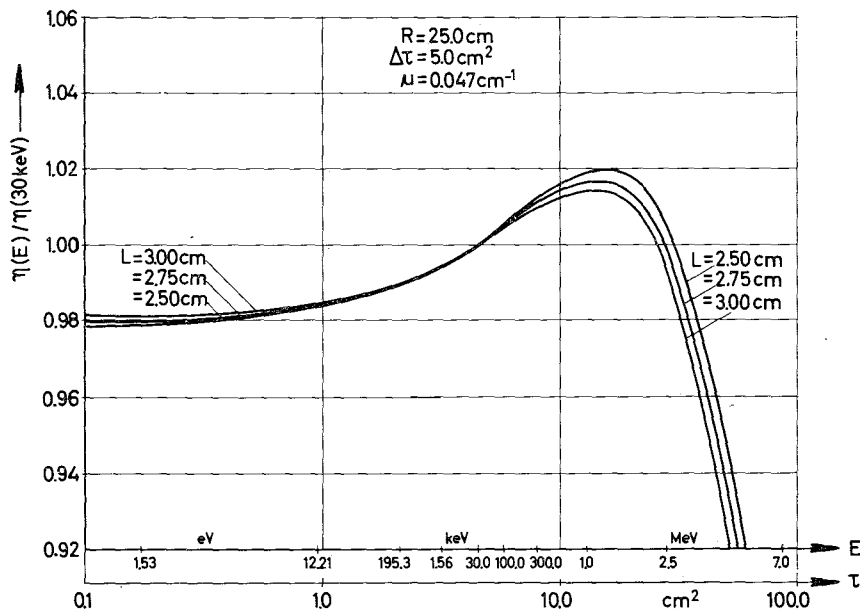


Fig. 5. The efficiency of the detector vs energy. The variable parameter is the diffusion length.

resonance and $\Delta\tau$ is the age from the indium resonance to thermal energy. For the following considerations we use $\tau_{1.44\text{eV}}$ of water as given by Goldstein et al.⁷). The difference between the slowing down age and the flux age is much too small to be important in the energy region of interest.

In fig. 3. the efficiency curves are shown for different radii R of the sphere. The increase of the efficiency for

higher neutron energy is due to the smaller γ -ray attenuation for capture γ -rays which originate on a larger mean radius than for primary thermal neutrons. The efficiency decrease at high energies is due to neutron leakage.

The influence of the parameter μ is shown in fig. 4. From the basic principle of the detector, it follows that for $\mu \rightarrow 0$ the efficiency curve is exactly flat in the region

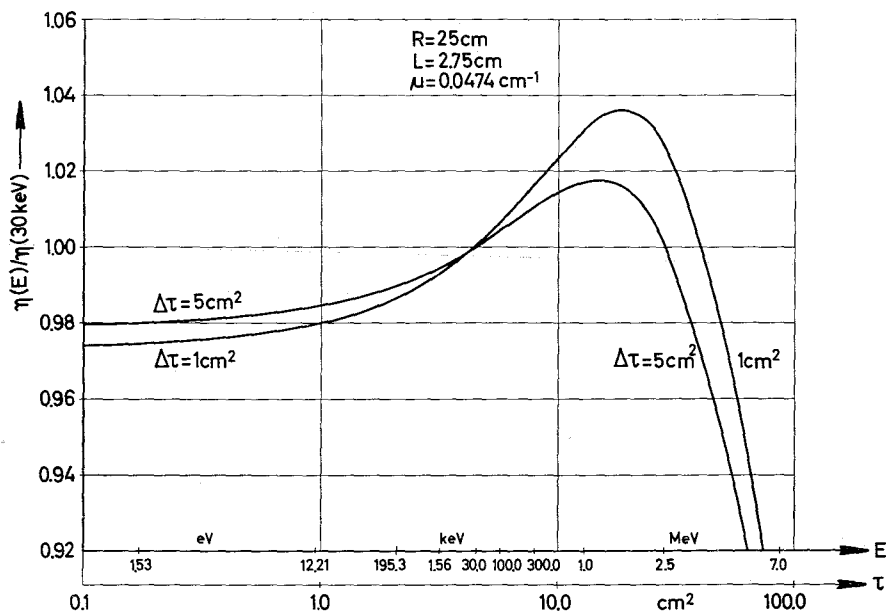


Fig. 6. The efficiency of the detector vs energy. The variable parameter is the neutron age $\Delta\tau$ from 1.44 eV to thermal energies.

where no leakage occurs. Therefore, the calculation of η for $\mu=0$ gives the leakage as determined by the $\phi_{th}(r)$ chosen for the calculation and the sphere radius R . Values of μ are available from theoretical calculations⁸) or they can be measured using radioactive γ -sources. There is an additional effect which should be considered. The energy loss of the γ -rays due to Compton scattering can be smaller than the resolution of the NaI(Tl)-detector. A decrease of 10% for the theoretical value of μ was calculated and this was found in agreement with our experimental determination of μ . In general, the uncertainty of μ should be less than 10%.

Figs. 5 and 6 show the efficiency curves for different values of L and $\Delta\tau$ respectively. As one can see, the influence of these parameters is small in the energy region where the neutron leakage is small. Values of L for water and paraffin have been measured very often and they are uncertain by only 1 or 2% [ref. 6), p. 368 and p.370]. A measured value⁹) of $\Delta\tau = 1.0 \pm 0.5 \text{ cm}^2$ is in relatively good agreement with a theoretical prediction of 0.8 cm^2 [ref. 6), p. 351].

5. The application of the detector

A possible arrangement for the use of the grey neutron detector in a neutron cross section experiment is shown in fig. 7. There should be a well collimated monoenergetic neutron beam which strikes the sample or the detector and enters into the grey neutron detector through a channel. The grey neutron detector should be

shielded by boron-paraffin to avoid the detection of background neutrons and the NaI(Tl) detector should be shielded by lead to reduce the background γ -radiation. However, the lead shielding should be positioned in such a way that the NaI(Tl) crystal can look at the whole paraffin sphere.

Comparing figs. 1 and 7 one can see that the realistic detector in fig. 7 violates one assumption used for the calculation of the efficiency curve. This is the isotropic distribution of source neutrons. First, there is the effect of the increase with increasing energy of the average path length for the first collision. The efficiency of the detector can be corrected by a factor

$$\{1 + (\Sigma_{30}R)^{-2}\} / \{1 + (\Sigma R)^{-2}\}, \quad (6)$$

where R is the radius of the sphere, $1/\Sigma$ the average path length and $1/\Sigma_{30}$ is the average path length for neutrons at the normalization point. Eq. (6) is valid for the arrangement shown in fig. 7 if one replaces the real neutron field by its center. The influence of the hole in the moderator (the channel in fig. 7) was investigated by placing an additional NaI(Tl) detector at 0° to the neutron beam direction and observing the counting ratios in the two detectors as a function of energy. In this experiment the moderator was a $60 \times 60 \times 60$ -cm paraffin pile with a $10 \times 10 \times 30$ -cm neutron entrance channel. No effect was found within the 2% counting statistics. Thus, the error resulting from this effect in

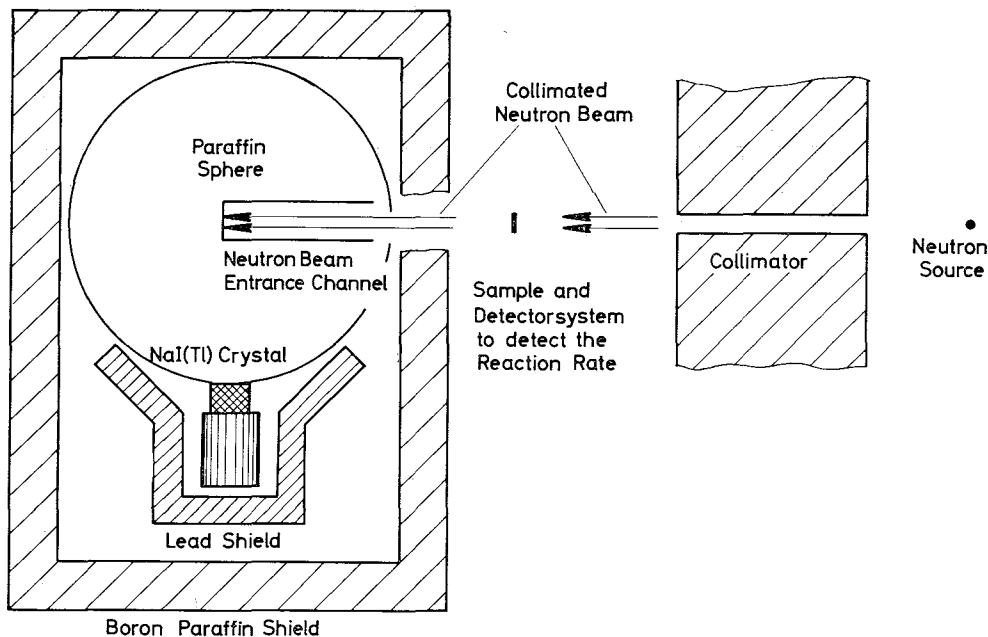


Fig. 7. Principle experimental setup for neutron cross section measurements using a "grey" neutron detector.

the NaI(Tl) detector at 90° should be less than 2%.

The use of a larger number of NaI(Tl)-detectors would increase the efficiency of the detector; however, it would not change the signal to room γ -radiation background ratio.

The energy range in which the grey neutron detector is applicable is given by the variation and certainty of the efficiency curve with the energy. It should be applicable from zero to a few hundred keV or a few MeV depending on the size of the detector.

It should be possible to measure with the arrangement shown in fig. 7 many kinds of cross sections where the "reaction method" [a separate determination of the neutron flux and the reaction rate, definition in ref. ¹⁰] is applicable. This concerns mainly fission and capture cross sections.

The capture cross sections of gold^{11,12}) and of uranium¹³) have been measured in the 25–500 keV energy range with an accuracy of about 5% using the grey neutron detector. A detailed description of these experiments will be given elsewhere^{12,13}).

The author wishes to acknowledge the help of Prof. Beckurts for interest in these investigations and Dr. H. O. Menlove and E. Wattecamps for interesting discussions.

References

- 1) A. O. Hanson and J. L. McKibben, *Phys. Rev.* **72** (1947) 673.
- 2) M. H. McTaggart, AWRE-Report NR/AL/59 (1958).
- 3) W. D. Allen, in *Fast Neutron Physics 1* (Interscience, New York, 1960) p. 361 and references cited therein.
- 4) D. W. Colvin and M. G. Sowerby, EANDC-33 "U" (1963) 44.
- 5) W. P. Pönitz and E. Wattecamps, *ibid.* 102.
- 6) K. H. Beckurts and K. Wirtz, *Neutron Physics* (Springer, Berlin, 1964).
- 7) H. Goldstein et al., ORNL-2639-34.
- 8) G. W. Grodstein, NBS Circular 583 (1956).
- 9) L. M. Barkow et al., *J. Nucl. Energy* **4** (1957) 94.
- 10) W. P. Pönitz, IAEA Conf. Paris 1966, *Nuclear Data for Reactors 1* (1967) 277.
- 11) W. P. Pönitz, IAEA Panel, Brussels (1967).
- 12) W. P. Pönitz et al., to be published (1967).
- 13) H. O. Menlove and W. P. Pönitz, to be published (1967).